

1
2
3
4 Development and Skill Assessment of a Real-Time Hydrologic-Hydrodynamic-Wave Modeling System for Lake Champlain
5 Flood Forecasting
6

7 Daniel Titze¹, Dmitry Beletsky², Jesse Feyen¹, William Saunders³, Lacey Mason¹, James Kessler¹, Philip Chu¹, Deborah Lee¹

8 ¹NOAA Great Lakes Environmental Research Laboratory, Ann Arbor, MI, USA
9

10 ²Cooperative Institute for Great Lakes Research, University of Michigan, Ann Arbor, MI, USA

11 ³NOAA National Weather Service Northeast River Forecast Center, Norton, MA
12

13 Corresponding Author:

14 Daniel Titze

15 dan.titze@noaa.gov

16 ORCID: 0000-0002-3412-8331
17
18
19

20 Keywords: Lake Champlain, hydrodynamic model, wave model, flood forecast
21
22
23

24 *Acknowledgements*

25 This work was funded by the International Joint Commission Lake Champlain-Richelieu River Study.

26 Funding was awarded to the Cooperative Institute for Great Lakes Research (CIGLR) through the NOAA Cooperative
27 Agreement with the University of Michigan (NA17OAR4320152). This is GLERL Contribution No. XXX and CIGLR
28 Contribution No. YYY.
29

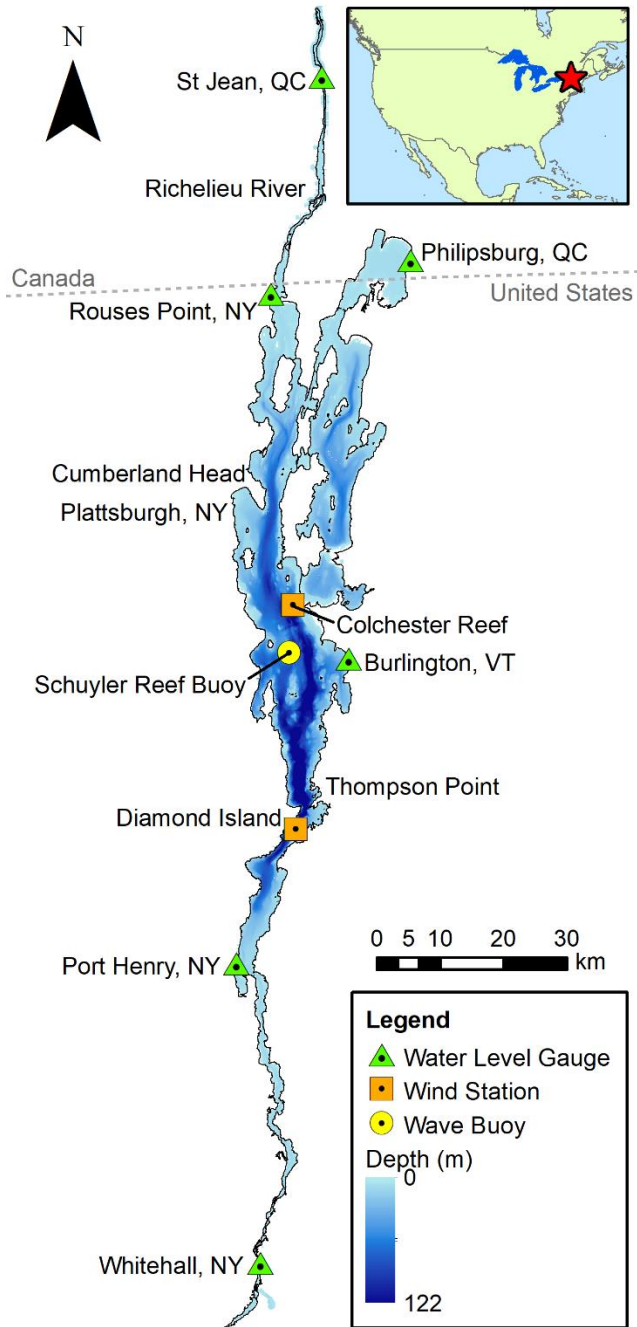
30
31 *Competing Interests*

32 The authors have no competing interests to declare that are relevant to the content of this article.
33
34
35
36

37 *Abstract*

38 In response to record-breaking flooding on Lake Champlain in 2011, the International Joint Commission launched a five-year
39 study to explore solutions to flooding in the binational Lake Champlain-Richelieu River (LCRR) basin. As a component of
40 the study, a real-time flood forecasting modeling system was developed to provide short-term (5-day) water level and wave
41 forecast guidance, intended to enhance flood preparedness by providing advanced warning of flooding to residents and other
42 stakeholders within the basin. The system consists of a hydrodynamic model built on the Finite Volume Community Ocean
43 Model (FVCOM) with one-way coupling to a WAVEWATCH III wave model. The National Water Model stream network
44 was expanded to include the entire LCRR domain, and is used to inform river inflows into the system. Water level output
45 from the hydrodynamic model shows strong agreement with gauge observations at annual and short-term time scales, with an
46 increasing negative bias at longer forecast horizons. Modeled significant wave heights compared well with observations
47 from a wave buoy deployed as part of the study, and also have a negative bias in the latter portions of the forecast. The scale
48 of the errors in modeled water levels and wave heights is consistent with an underestimation of river inflow and wind speed
49 inputs, respectively, based on validation of these model forcings against available observations. The development and
50 validation of the LCRR modeling system serves as a precursor for the first operational real-time 3D hydrodynamic-wave
51 forecast system for Lake Champlain.
52
53
54
55
56
57
58
59
60
61
62
63
64
65

1
2
3
4 1. Introduction
5
6



51
52 **Fig. 1** Overview Map. Map of Lake Champlain and the upper Richelieu River, showing the location of the lake, the lake
53 bathymetry, water level gauges (triangles), wind stations (squares), and wave buoy (circle)

54 Lake Champlain is a binational lake, located between the United States (US) states of New York (NY) and Vermont (VT),
55 and extending northward into the Canadian province of Québec (QC). The lake is deep and narrow, with a north-south length
56 of approximately 193 km, a maximum width of approximately 19 km, and a maximum depth of 122 m (Fig. 1) (Stickney et
57 al. 2001). The southern portions of the basin are characterized by steep bathymetry, with the Adirondack Mountains of NY
58 to the west and the Green Mountains of VT to the east, while the northern portions are flatter. The area of the Lake
59 Champlain watershed (21,326 km²) is approximately 19 times larger than the lake surface area (1,127 km²). Water from
60
61

1
2
3
4 Lake Champlain flows northward through the Richelieu River beginning near Rouses Point NY, where it eventually enters
5 the St. Lawrence Seaway. Due to its temperate location, Lake Champlain forms partial to full ice cover each winter.
6

7 The mountainous setting and large catchment area of Lake Champlain make the basin hydrologically flashy and prone to
8 flooding. In the spring of 2011, Lake Champlain experienced record flooding when rapid snow melt and heavy spring rains
9 combined to generate a rapid rise in lake levels (Riboust and Brissette 2016). The lake was above the US National Weather
10 Service (NWS) flood stage for 67 days, from April 13 through June 19, and experienced the highest lake levels since record-
11 keeping began in 1827 (Bjerklie et al. 2014). Damage was made worse by high winds during the flood, which produced
12 waves that caused damage and erosion up to 1.5 m above the record lake levels (LCBP 2013). The flooding led to evacuation
13 of residents along the lake shore, with damages in excess of 82 million US dollars throughout NY, VT, and QC (ILCRRSB
14 2019). Later the same year, on August 28, Tropical Storm Irene produced high winds and rain totals of more than 20 cm over
15 24 hours in the Lake Champlain Basin, leading to a rapid 1-m rise in water levels (LCBP 2013), and there are indications that
16 such extreme events are occurring with increasing frequency due to climate change (Riboust and Brissette 2015).
17
18

19 In 2016, the International Joint Commission (IJC) began a 5-year study at the request of the US and Canadian governments to
20 explore solutions to flooding in the binational Lake Champlain-Richelieu River (LCRR) system (ILCRRSB 2019). The final
21 report from the study was released in 2022, and included the recommendation that “For short term forecasts out to five days,
22 wind and wave effects on Lake Champlain water levels must be included in lake level predictions” (ILCRRSB 2022). As a
23 component of the IJC LCRR study, we completed development and validation of a linked hydrologic-hydrodynamic-wave
24 real-time flood forecast modeling system for the LCRR domain (Beletsky et al. 2022). The goal of the modeling system is to
25 provide forecasters with improved guidance on water levels and waves throughout the domain, and ultimately to enhance
26 flood preparedness by providing advanced warning of flooding to residents and other stakeholders within the basin. The
27 LCRR modeling system consists of a three-dimensional (3D) hydrodynamic model with one-way coupling to a spectral
28 surface wave model. The use of 3D coastal ocean models represents a major advancement in real-time flood forecasting
29 within the basin, as the current modeling system used by US forecasters in the region is based upon a one-dimensional (1D)
30 Hydrologic Engineering Center-River Analysis System (HEC-RAS) model, which does not simulate wind-driven storm
31 surges or waves on the lake.
32
33
34

35 Hydrodynamic modeling in Lake Champlain dates back to the 1990s, where early hydrodynamic models were developed to
36 support management decisions relating to phosphorus dynamics and sediment transport (Campbell and White 2020;
37 Mendelsohn et al. 1995, 1997). More recently, 3D hydrodynamic models have been developed for Lake Champlain using the
38 MIKE 3, D-Flow Flexible Mesh, and Aquatic Ecosystem Model 3D software packages, with goals of assessing sediment
39 transport, characterizing lake circulation and temperature dynamics, and understanding nutrient cycling and the occurrence of
40 harmful algal blooms within the lake (Campbell and White 2020; Herdman et al. 2019; Marti et al. 2019). As a part of the
41 IJC LCRR study, Environment and Climate Change Canada (ECCC) developed a two-dimensional hydrodynamic (H2D2)
42 model of Lake Champlain, which was designed to characterize flood zones and assess the impacts of potential flood
43 scenarios and mitigation measures (Boudreau et al. 2015). Little attention has been paid to wave modeling on Lake
44 Champlain, and no real-time 3D hydrodynamic modeling system exists for the basin.
45
46
47

48 Operational 3D hydrodynamic modeling systems have been developed for many coastal regions of the US (Peng et al. 2014;
49 Wei et al. 2014), as well as for all five of the Great Lakes (Anderson et al. 2018; Chu et al. 2011; Kelley et al. 2018). In
50 addition, real-time wave models exist for the global ocean and the Great Lakes (EMC 2022). However, such operational
51 systems are far less common in smaller inland lakes, and the steep bathymetry and narrow morphology of Lake Champlain
52 make it a uniquely challenging setting for the application of oceanographic models. Hydrodynamic models developed for the
53 coastal ocean and the Great Lakes typically end at the shoreline, limiting their usefulness for flood forecasting. Furthermore,
54 wave modeling is often done separately from hydrodynamic modeling with an assumption of nominal lake conditions, such
55 that the impacts of rising and falling water level near the shoreline are not represented in the wave model and no waves form
56 in flooded areas. This LCRR modeling system applies oceanographic approaches to a flood-prone inland lake system,
57 expanding the domain into the floodplain to support dynamic inundation, and establishing a one-way coupling framework
58
59
60
61
62
63
64
65

1
2
3
4
5
6
7
8
9
10
11
12
13
14
15
16
17
18
19
20
21
22
23
24
25
26
27
28
29
30
31
32
33
34
35
36
37
38
39
40
41
42
43
44
45
46
47
48
49
50
51
52
53
54
55
56
57
58
59
60
61
62
63
64
65

such that predicted changes in water level and inundation area are incorporated into the wave model. This system will benefit forecasters by simulating and predicting the full range of flood impacts along the coast.

2 Methods

2.1 Modeling system overview

The LCRR modeling system consists of a hydrodynamic model and a wave model that are linked through a one-way coupling setup, whereby water level output from the hydrodynamic model is used as input to the wave model. The LCRR modeling system is configured to function as an operational forecasting system, such that it can reliably deliver results in near-real-time. The model setup and validation presented in this paper are designed to simulate and assess the performance of the modeling system in a pseudo-operational environment. The pseudo-operational framework consists of a nowcast cycle that updates every 6 hours, and a 5-day forecast cycle that initiates daily, using the corresponding nowcast results as initial conditions. Both the nowcast and forecast cycles produce instantaneous hourly estimates of water levels, water currents, and waves throughout the domain.

1
2
3
4
5
6
7
8
9
10
11
12
13
14
15
16
17
18
19
20
21
22
23
24
25
26
27
28
29
30
31
32
33
34
35
36
37
38
39
40
41
42
43
44
45
46
47
48
49
50
51
52
53
54
55
56
57
58
59
60
61
62
63
64
65

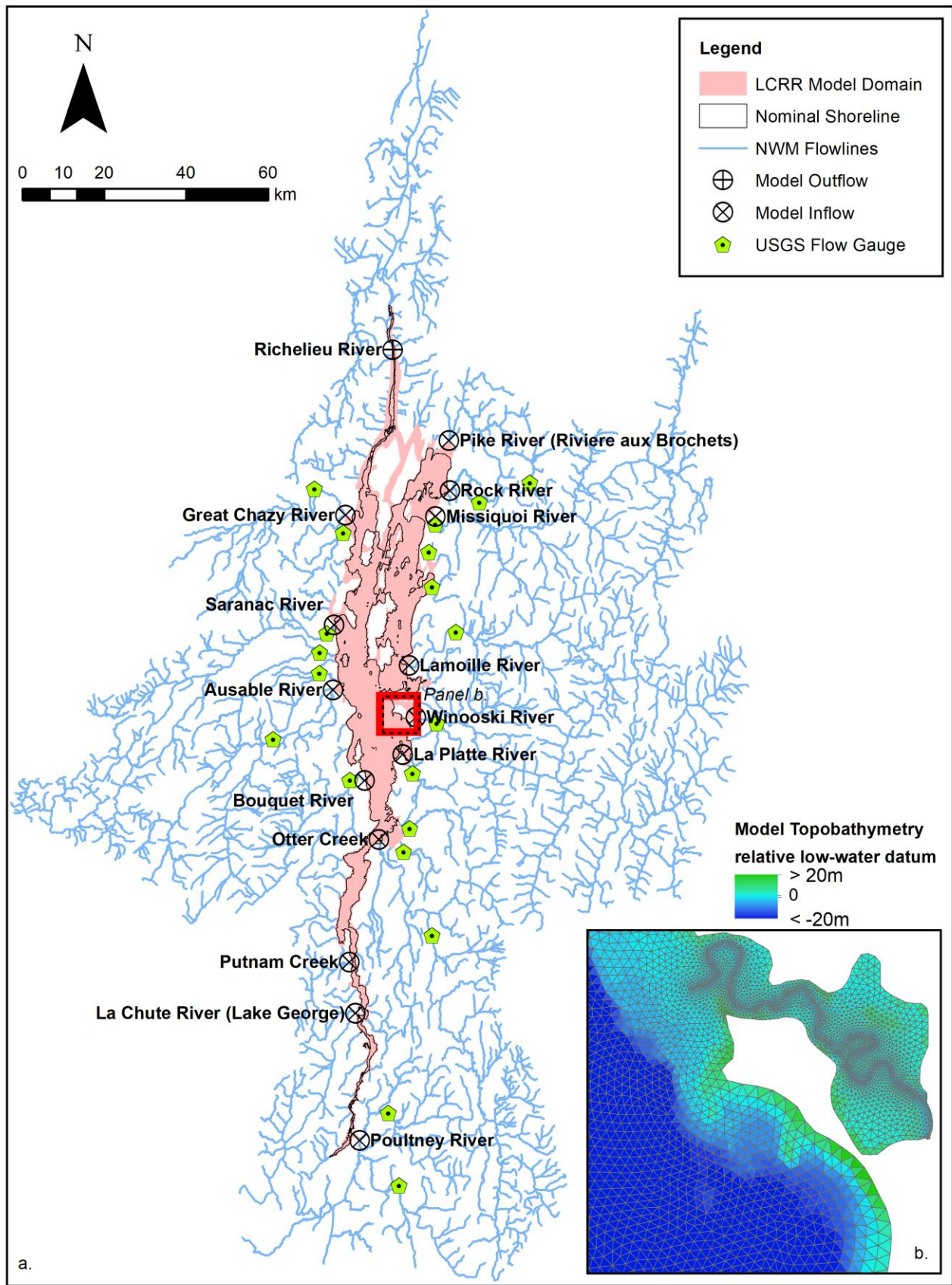


Fig. 2 Model domain. (a) The LCRR model domain (shaded), along with river inflows (circles with X) and outflow (circle with +) incorporated in the model. Stream segments depicting the expanded NWM coverage for the LCRR watershed are shown (line segments), along with USGS streamflow gauges used to validate the NWM (pentagons). (b) An inset showing the mesh resolution and topobathymetry for Burlington VT and the Winooski River

The LCRR model domain includes Lake Champlain, the upper Richelieu River, and the surrounding floodplain (Fig. 2). The topobathymetric grid used in the LCRR modeling system was derived by downscaling the mesh developed by ECCC for use in a high-resolution, two-dimensional hydrodynamic model, which compiled and unified topobathymetric data from 15 sources (Boudreau et al. 2015). Coverage extends southward to South Bay and the Poultney River at Whitehall NY, and northward to Fryers Rapids, just downstream of St Jean QC, and spatially resolves 14 major river inflows to the lake. The extent of surrounding floodplain included in the mesh is designed to accommodate inundation scenarios for the full range of water level conditions experienced within the domain. The LCRR grid contains 61,332 triangular elements, typically ranging in size from 50 m in coastal areas to 400 m in the open lake, with isolated areas as fine as 18 m and as coarse as 669 m (Fig. 2b).

The LCRR modeling system uses the North American Vertical Datum of 1988 (NAVD88) as its vertical datum for reporting water level output and interfacing with gauge observations. Gauge data is from the US Geological Survey (USGS 2022) and from ECCC (ECCC 2022). Water level data from gauges throughout the lake were unified onto the NAVD88 datum according to the datum harmonization surveys conducted by USGS for the Lake Champlain basin (Flynn et al. 2016). Water level station information, including station-specific vertical datum conversions, is presented in Table 1.

Nominal Location	Source	Station ID	Longitude (deg E)	Latitude (deg N)	Source Datum	Conversion to NAVD88 (m)
Whitehall, NY	USGS	04279085	-73.4189	43.6217	NGVD29	-0.082
Burlington, VT	USGS	04294500	-73.2219	44.4761	NGVD29	-0.159
Rouses Point, NY	USGS	04295000	-73.3603	44.9961	NGVD29	-0.131
Philipsburg, QC	ECCC	02OH001	-73.0797	45.0397	Station-Specific (CGVD28 - 24.384m)	24.319
Port Henry, NY	USGS	04294413	-73.4533	44.0525	NGVD29 (2015-pres) NAVD88 (2019-pres)	N/A
St Jean, QC	ECCC	02OJ016	-73.2500	45.3023	Station-Specific (CGVD28 - 28.301m)	28.282

Table 1 Water Level Gauges. Summary of water level gauges, including the nominal location used to refer to the station, the source agency and station identification, the geographic coordinates of the station, the vertical datum used in the originating data source, and constant value added to the origin data to harmonize to NAVD88

2.2 Hydrodynamic model setup

The LCRR hydrodynamic model is built upon the Finite-Volume Community Ocean Model (FVCOM) version 4.3.1. FVCOM is a prognostic, unstructured-grid, finite-volume, free-surface, 3-D primitive equation coastal ocean circulation model that produces a computationally-efficient numerical solution to the integral form of the governing equations using a second-order accurate discrete flux calculation (Chen et al. 2006, 2013). The FVCOM model formulation is configured for an unstructured triangular grid with terrain-following sigma vertical coordinates, and employs a dynamic point-based wetting and drying parameterization to simulate flooding in the coastal floodplain. The flexibility and efficiency of the model configuration has led to widespread usage in operational systems for applications in both the coastal ocean (Peng et al. 2014; Wei et al. 2014) and the Great Lakes (Anderson et al. 2018; Kelley et al. 2018, 2020). The LCRR FVCOM model is run in a

1
2
3
4 3D barotropic mode, with a spherical horizontal grid, 21 uniform sigma levels in the vertical, and utilizing FVCOM's
5 dynamic wetting and drying module for floodplain regions. Based on initial calibration and stability testing, a uniform
6 bottom roughness length-scale of 2.5 cm is used, and an external integration timestep of 0.5 sec is used.
7

8 River inflow data is from the National Oceanic and Atmospheric Administration (NOAA) National Water Model (NWM).
9 The NWM is a data-assimilating hydrologic modeling framework that provides forecasts of streamflow throughout the
10 continental US (Cosgrove et al. 2016; OWP 2022). The operational implementation of the NWM at the beginning of the
11 LCRR study was version 2.0, which did not have coverage of the Canadian portion of the Lake Champlain watershed. As a
12 component of the LCRR study, the NWM domain was expanded to include these areas, thus filling a critical gap in the
13 hydrologic representation of the basin. To facilitate this expansion, a moderate-resolution hydrofabric was developed based
14 on the 1:100,000 scale NHDPlus V2 dataset (McKay et al. 2012), and this upgrade was incorporated in operational version
15 2.1 of the NWM, released in April 2021 (Fig. 2a). Given that approximately 12.5% of the Lake Champlain watershed is
16 ungauged (Boudreau et al. 2015), the NWM domain expansion supports the need for a comprehensive accounting of
17 hydrologic inputs into the LCRR model, as well as providing forecasts for these flows, which are not available through
18 observational platforms.
19
20

21
22 River inputs into the hydrodynamic model are applied as volumetric fluxes as the boundaries of the model domain, using
23 streamflow data from the NWM analysis (0-hour horizon), short-term forecast (18-hour horizon), and medium-term forecast
24 (10-day horizon) models. All 73 of the NWM inflows within the Lake Champlain basin are configured as inputs into the
25 LCRR model. Because many of these inflows are too small to be spatially resolved within the model grid, inflows are
26 aggregated and applied at the nearest of the 14 fully-resolved major inflows (Fig. 2a). This ensures that the total inflow
27 volume from the NWM is being applied in the model with a realistic spatial distribution, thus preserving both the basin-scale
28 hydrology and subbasin-scale dynamics within the system.
29

30
31 There is a delay in the availability of NWM data as a result of the system's operational data flow. The NWM analysis model
32 is updated hourly with a delay in availability of approximately 1 hour, the NWM short-range forecast is initiated hourly with
33 a delay in availability of approximately 2 hours, and the NWM medium-range forecast is initiated every 6 hours with a delay
34 in availability of approximately 6 hours. The real-time configuration of the LCRR modeling system incorporates a delay in
35 model initiation to account for these delays in NWM data availability. The hydrodynamic nowcast cycle is delayed by 80
36 minutes to ensure availability of corresponding NWM analysis data. The hydrodynamic forecast cycle is delayed by 140
37 minutes and uses the NWM analysis model for hours 0-1 of the forecast, the NWM short-range forecast for hours 2-18 of the
38 forecast, and hours 25-126 of the 6-hour-old NWM medium-range forecast for the remainder of the hydrodynamic forecast.
39 This configuration was chosen to balance the timeliness of results with the accuracy of forcing.
40

41
42 The Richelieu River is the outflow from the LCRR domain, and is applied as an elevation open-boundary condition in the
43 model using data from ECCC water level gauge 02OJ016 in St Jean QC. Because no source of forecast data has been
44 identified for the Richelieu River, the elevation at the open boundary throughout the 5-day forecast window is estimated by
45 persisting the last available measurement at the time the forecast model is initiated. The NWM was also evaluated as a
46 potential source of streamflow data for the Richelieu River outflow; however, it was found that the NWM has inadequate
47 skill at the outflow location, likely due to the simplified treatment of Lake Champlain as a simple reservoir, thus precluding
48 its use.
49

50
51 Atmospheric forcing for the LCRR hydrodynamic model is obtained from the NOAA High-Resolution Rapid Refresh
52 (HRRR) for hours 0-48 of the forecast (Dowell 2022; GSL 2022; James 2022) and from the NOAA Global Forecasting
53 System (GFS) operational models for hours 48-120 of the forecast (NCEI 2022). This configuration was chosen because
54 HRRR winds were identified to have higher resolution and accuracy than GFS in preliminary assessments, but HRRR
55 forecasts only extend 48 hours into the future, thus necessitating the use of GFS for the remainder of the desired 5-day
56 forecast window. The National Digital Forecast Database (NDFD) was also considered as a potential operational source of
57 atmospheric forcing data for the modeling system, but was disqualified because it does not include the Canadian portion of
58 the LCRR domain. While the combined HRRR-GFS results in a discontinuity in forcing, the benefits of more accurate wind
59 forcing during the early portion of the forecast are believed to outweigh any drawbacks to this approach, and no detrimental
60
61
62
63
64
65

1
2
3
4 effects of the forcing discontinuity have been identified in the model output. Forcing data used in the nowcast cycle are
5 compiled from hour 1 of the HRRR forecasts.
6

7 Atmospheric forcing parameters to the FVCOM model include wind and overlake precipitation. Forcing parameters were
8 interpolated from their native grid to the model grid using bilinear interpolation, using the Universal Transverse Mercator
9 Zone 18N (UTM18N) projection as the cartesian interpolation space, with winds interpolated by speed and direction. It was
10 found that precipitation can produce instabilities in FVCOM when applied to dry areas of the domain, so all precipitation
11 forcing is applied only to the main water body. This is accomplished through a preprocessing method that masks
12 precipitation in any grid nodes that are shallower than 1 m at the beginning of the run, as well as in any ponded areas that are
13 disconnected from the main water body.
14

15
16 A water level nudging method was implemented to keep the lake stage from drifting over time due to imperfect forcing and
17 hydrodynamics in the model. As a pre-processing step for each nowcast and forecast cycle, the water level drift from the
18 previous 6-hourly nowcast cycle is calculated, and a commensurate volume of water is added or removed to offset this drift.
19 The drift is calculated as the median difference between modeled and observed water level at five water level stations
20 distributed throughout the basin, including Whitehall NY, Port Henry NY, Burlington VT, Philipsburg QC, and Rouses Point
21 NY (Fig. 1, Table 1). The nudge is applied in FVCOM as evenly-distributed precipitation or evaporation over the main water
22 body over the first 6 hours of model run.
23
24
25

26 27 2.3 Wave Model Setup

28 The LCRR surface wave model is built upon the WAVEWATCH III (WW3) community wave modeling framework version
29 6.07 (WW3DG 2019). WW3 is a non-phase-resolving spectral wave model developed at NOAA National Centers for
30 Environmental Prediction (NCEP) that solves the random phase spectral action density balance equation for wavenumber-
31 direction spectra. It is well-suited for wave simulations in coastal environments, and incorporates parameterizations for
32 coastal processes such as refraction and straining due to spatial variations in depth, as well as several growth and decay
33 processes, and dynamic wetting and drying in floodplain areas. WW3 includes formulations for unstructured grids, and for
34 both explicit and implicit solvers.
35
36

37 Wind forcing for the LCRR wave model was obtained from the HRRR and GFS atmospheric models, consistent with
38 atmospheric forcing used in the FVCOM hydrodynamic model and using the same methods of interpolation (Section 2.2).
39

40 Because Lake Champlain is a temperate lake that forms some degree of ice cover each winter and ice cover damps surface
41 waves, it is important the ice cover be considered in the LCRR wave model. Ice cover datasets for Lake Champlain are
42 sparse, and no suitable operational dataset was identified for use in the LCRR modeling system. However, the NWS Weather
43 Forecast Office in Burlington VT (WFO Burlington) maintains an ice mask for Lake Champlain throughout the winter season
44 that may serve as a dataset of opportunity for the LCRR modeling system. The ice mask has a resolution of 2.5 km and is
45 manually produced by a technician based on the most recent clear-sky satellite image. The US National Ice Center Ice
46 Mapping System operational daily 1-km northern hemisphere snow and ice analysis (USNIC 2008) was also evaluated as a
47 possible data source for Lake Champlain ice cover; however, it was found that the 1-km dataset uses a 4-km land mask for
48 Lake Champlain and does not have adequate spatial resolution or accuracy to be used in the LCRR modeling system.
49

50
51 Methods were developed for incorporating the WFO Burlington ice dataset into the LCRR wave model using a simple ice
52 blocking (IC0) parameterization (WW3DG 2019). The IC0 parameterization uses a binary presence or absence treatment of
53 ice cover, whereby areas of the model domain with ice cover are treated as land in model calculations. While the WFO
54 Burlington IC0 parameterization was tested as a prototype for incorporation of ice data into the LCRR wave model, it is
55 discussed primarily to document the current state of ice data availability for Lake Champlain. All model validation was
56 conducted during ice-free conditions, due to the seasonal availability of wave observations, and wave-ice interactions are not
57 further considered here.
58
59
60
61
62
63
64
65

1
2
3
4 Spatially-variable water level data for the wave model is ingested from the FVCOM hydrodynamic model using a linked one-
5 way coupling setup. This approach is designed to improve representation of water depths, particularly in shallow coastal
6 areas, and to simulate and forecast which areas of the domain are inundated, such that the model produces waves in flooded
7 areas. For each nowcast or forecast cycle, the wave model component is not initiated until the corresponding hydrodynamic
8 component has completed. Instantaneously hourly water level output from the hydrodynamic model are formatted as input
9 forcing for the wave model as part of pre-preprocessing. Because both the FVCOM hydrodynamic model and the WW3
10 wave model are run on the same unstructured triangular grid, no interpolation is necessary to transfer data between the
11 models. Although WW3 has the capability to dynamically simulate wetting and drying based on water level forcing, dry
12 areas are masked in the FVCOM output, so information on floodplain wetting and drying is explicitly forced in the wave
13 model according to the results of the corresponding hydrodynamic model run.
14
15
16
17

18 2.4 Model Skill Assessment

19 2.4.1 Skill Assessment Overview

20 Model skill assessment was conducted for the period of May 2021 through April 2022. This period was chosen as a complete
21 year during which there is data coverage for the best-available forcing and validation data. The current version of the NWM
22 at the time of this writing is version 2.1, which was released in April 2021, and the current version of HRRR at the time of
23 this writing is version 4, which was released in December 2020. Conducting the skill assessment after the implementation of
24 these upgrades ensures that the improvements to these forcing models are integrated into the LCRR hydrodynamic and wave
25 model results, and that the corresponding skill assessment is representative of the performance of the model under the
26 configuration described herein. Furthermore, assessing the model skill over a complete year helps mitigate any bias toward a
27 particular season in the skill statistics.
28
29
30
31

32 Skill assessment was conducted to validate river forcing from the NWM hydrologic model, wind forcing from the HRRR and
33 GFS atmospheric models, water level results from the FVCOM hydrodynamic model, and wave results from the WW3 wave
34 model. As necessary to span the 120-hour forecast horizon, datasets used for forcing validation were compiled from multiple
35 sources consistent with the configuration of the LCRR real-time modeling system (e.g. short-term and medium-term NWM
36 forecasts; HRRR and GFS forecasts). The primary goal of these analyses is to quantify the error in the datasets used to force
37 the models, and not necessarily to provide a comprehensive assessment of the source models. However, to our knowledge,
38 no skill assessment of the NWM, HRRR, or GFS models have been conducted specific to the Lake Champlain basin, and
39 results from these analyses will additionally provide insight into the performance of these operational models in the region.
40
41

42 Differences between model results and observations were quantifying using a combination of linear regression, root mean
43 square error (RMSE), and mean bias error (MBE), where RMSE and MBE are calculated as:

$$44 \quad RMSE = \sqrt{\frac{\sum_{i=1}^n (\hat{x}_i - x_i)^2}{n}} \quad \text{Eqn. 1}$$

$$45 \quad MBE = \frac{\sum_{i=1}^n (\hat{x}_i - x_i)}{n} \quad \text{Eqn. 2}$$

46 Where n is the number of data points, \hat{x} is the modeled value, and x is the observed value.
47
48
49
50
51
52
53

54 2.4.2 River Inflows

55 Observations of streamflow were used to validate the streamflow simulations produced by the NWM. Streamflow
56 observations used in this analysis were from 20 USGS gauges throughout the Lake Champlain basin, which are shown in
57 Figure 2a. A maximum of one gauge per river subbasin was used in this analysis so as not to unduly weigh results toward
58 any particular river. For river subbasins that have more than one gauge, the most downstream gauge was used. The
59
60
61
62
63
64
65

1
2
3
4 corresponding NWM stream features used for validation are those containing each respective USGS stream gauge. In many
5 cases, NWM stream features used for validation are different from those features used to force the hydrodynamic model,
6 because many gauges are located upstream from the lake inflow.
7

8 Skill assessments were conducted to assess the accuracy of river forcing for both the nowcast and forecast cycles. The
9 nowcast skill assessment was conducted by comparing observation from USGS stream gauges to results from the NWM
10 analysis model. Forecasts of river data used for the skill assessment were assembled by combining data from the NWM
11 analysis, short-range forecast, and 6-hour-old medium range forecast models, as described in Section 2.2, such that the
12 datasets used in the skill assessment are consistent with the datasets used to force the hydrodynamic model. Comparisons
13 were made between observed and modeled streamflow for all hourly data points within the skill assessment period for which
14 observations from the relevant gauge were available.
15
16
17
18

19 2.4.3 Wind

20
21 Wind observations from the Forest Ecosystem Monitoring Cooperative (FEMC) were used to validate the HRRR and GFS
22 atmospheric models in terms of both wind speed and direction (FEMC 2022). The FEMC maintains three wind stations
23 within Lake Champlain, with locations at Burton Island, Colchester Reef, and Diamond Island. Data from the Colchester
24 Reef and Diamond Island stations were used in the skill assessment (Fig. 1), while Burton Island was excluded from the
25 analysis because the station is partially sheltered by trees and does not contain data for the duration of the skill assessment
26 period. The Colchester Reef and Diamond Island stations are positioned at heights of 10m and 17m above lake level,
27 respectively. Wind observations from Diamond Island were scaled to a standard height of 10m above the lake level using the
28 wind profile power law under a neutral stability assumption (Touma 1977). Wind observations from the Colchester Reef and
29 Diamond Island stations are available year-round, with 91.8% and 99.3% hourly data coverage over the May 1, 2021 to May
30 1, 2022 skill assessment period, respectively. Consistent with the configuration of the LCRR models, skill assessment for the
31 nowcast was conducted using data from the 1-hour forecast horizon in the HRRR model, and skill assessment for the forecast
32 was conducted using data from the HRRR for the first 48 hours and from the 6-hour-old GFS for the remainder.
33
34
35
36
37

38 2.4.4 Water Level

39 Water level results from the FVCOM hydrodynamic model were validated against water level observations from five water
40 level gauges throughout the lake. The gauges used for validation are the same five gauges used in the FVCOM nudging
41 calculation (Section 2.2; Fig. 1; Table 1). Hourly data from the gauge timeseries were subset and compared to instantaneous
42 hourly output from the hydrodynamic model. Skill statistics calculated for validation integrate both the performance of the
43 nudging process in tracking the lake stage, as well as the model's capability of capturing spatial fluctuations in water level
44 due primarily to wind influence on the lake.
45
46
47
48

49 2.4.5 Waves

50 Wave data on Lake Champlain are historically sparse. As a component of the LCRR study, the NOAA Great Lakes
51 Environmental Research Laboratory, in collaboration with the University of Vermont and the Coastal Data Information
52 Program, deployed a Datawell Directional Waverider 4 (DW4) buoy in Lake Champlain. The DW4 has a data output rate of
53 2.56 Hz; it measures wave heave at 1 mm precision with accuracy of 0.5% of the measured value, and wave direction with
54 0.1° precision with accuracy of 0.4 to 2°. The DW4 buoy was deployed in the main basin of the lake near Schuyler Reef,
55 with approximate coordinates 44.4877° N and 73.3391° W (Fig. 1). This location was chosen because it is in the open lake
56 with the potential for long wind fetch and large waves, and is in a region of the lake with elevated human activity, including a
57 nearby commercial ferry route and recreational boat traffic from the population center of Burlington VT.
58
59
60
61
62
63
64
65

1
2
3
4
5
6
7
8
9
10
11
12
13
14
15
16
17
18
19
20
21
22
23
24
25
26
27
28
29
30
31
32
33
34
35
36
37
38
39
40
41
42
43
44
45
46
47
48
49
50
51
52
53
54
55
56
57
58
59
60
61
62
63
64
65

The buoy was deployed for the 2021 ice-free season from May 10 to October 18, which will serve as the skill assessment period for the wave model. These are the only known in-situ wave observations in Lake Champlain for 2021, and represent the best available source of wave observations for use in model validation. An hourly subset of measurements of significant wave height and wave direction were compared to corresponding model results over the period of analysis.

3. Results

3.1 River Inflow Validation

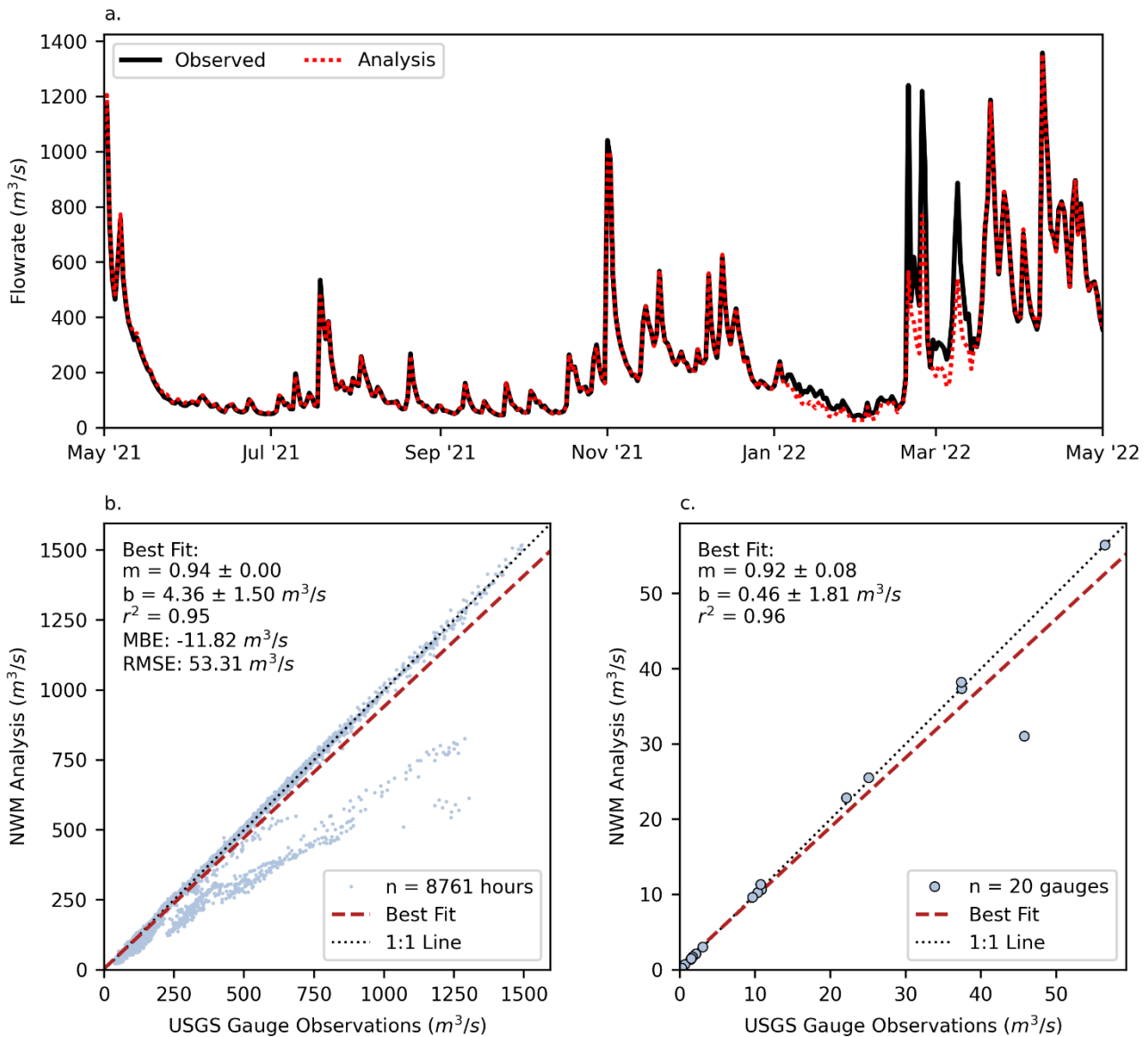


Fig. 3 River Inflow Nowcast Skill Assessment. (a) Time-series of daily total inflow rate from 20 tributaries from gauge observations (solid) and the NWM analysis model (dashed) over the skill assessment period. (b) Linear regression of hourly total inflow values from 20 tributaries from the NWM analysis model against gauge observations, including hourly data points and best fit line. (c) Linear regression of average streamflow over the skill assessment period for each of the 20 tributaries for the NWM analysis model against gauge observations, with one data point for each tributary and an overall best fit line

Combined inflow values of the 20 tributaries analyzed in the skill assessment show generally strong agreement between the NWM and USGS gauge observations (Fig. 3a-b), with an r^2 value of 0.95 and a best-fit slope of 0.94 ± 0.00 . The NWM has a MBE of $-11.8 \text{ m}^3/\text{s}$ and a RMSE of $53.3 \text{ m}^3/\text{s}$; when scaled to the average combined inflow of these features during the skill assessment period ($254.5 \text{ m}^3/\text{s}$), the relative MBE and RMSE are -4.6% and 20.9% , respectively. When analyzed separately

by river (Fig. 3c), 19 of the 20 rivers show strong agreement with observations, while NWM results show noticeable differences from observations in one river (the Lamoille River); the overall r^2 value of the by-river nowcast analysis 0.96 and the best-fit slope is 0.92 ± 0.08 . The high degree of skill in the NWM nowcast model is expected, because it incorporates an aggressive data assimilation process, such that streamflow values in features with gauges are tuned to match values reported by the gauges when present.

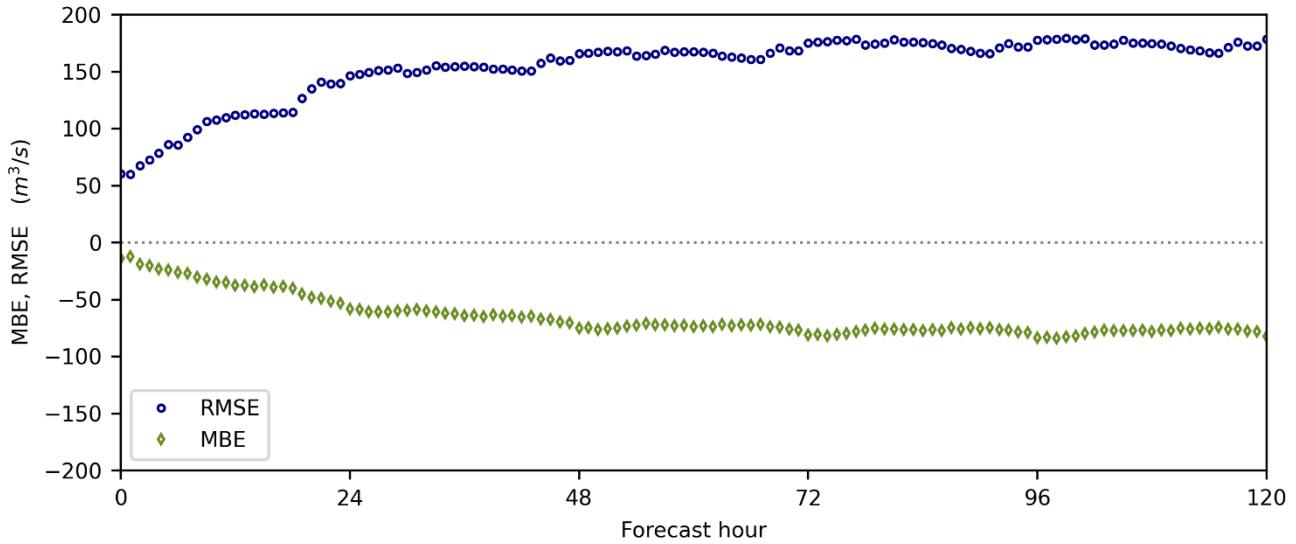


Fig. 4 River Inflow Forecast Skill Assessment. RMSE (circles) and MBE (diamonds) for the total inflow of 20 tributaries by forecast horizon, calculated by compared river forecasts derived from NWM short-term and medium-term forecasts to gauge observations

The NWM forecast skill was assessed by forecast horizon, with skill statistics calculated and plotted for each hourly forecast horizon (Fig. 4). Results from the skill assessment demonstrate a steeper decline in skill over approximately the first 24 hours of the forecast, followed by more gradual declines in skill up to approximately day 3 of the forecast, with minimal declines in skill over the remainder of the 5-day forecast. At a forecast horizon of 120 hours, the forecast has a MBE of -82.11 m³/s, and a RMSE of 178.65 m³/s; when scaled to the average total flow of these rivers at the times analyzed (258.66 m³/s), the relative MBE and RMSE are -31.7% and 69.1%, respectively. As is apparent in the time-series of select forecast horizons, larger streamflow events are typically underpredicted at longer forecast horizons, consistent with an increasing negative MBE at longer forecast horizons.

Streamflow values for the Lamoille River in the NWM at times noticeably deviated from observations. Of the 20 gauged features included in this analysis, the Lamoille River is the second largest by average inflow, representing approximately 18% of the combined inflow. Review of the data files for the USGS Lamoille River gauge 0429500 revealed that it experienced icing and equipment malfunction between approximately December 26, 2021 and March 16, 2022, during which real-time data for the station were not available. The USGS has since published quality-controlled estimated flow rates for this period. There is a consistent negative bias in the NWM nowcast values throughout this period, which is most pronounced during high-flow events on February 19, February 24, and March 9, for which the NWM response is greatly muted relative to USGS gauge data.

Because, necessarily, all features analyzed in this skill assessment are gauged, results are representative of the capability and reliability of the NWM at locations within the LCRR domain heavily influenced by the data assimilation component of the NWM. Results from the NWM nowcast analysis demonstrate that forcing data obtained from the model is generally highly consistent with gauge observations, though the skill of the NWM in the region may be reduced when there are outages in the data sources it assimilates. Since such lapses in NWM accuracy occur as a direct result of gauge outages, and real-time

1
2
3
4
5
6
7
8
9
10
11
12
13
14
15
16
17
18
19
20
21
22
23
24
25
26
27
28
29
30
31
32
33
34
35
36
37
38
39
40
41
42
43
44
45
46
47
48
49
50
51
52
53
54
55
56
57
58
59
60
61
62
63
64
65

gauge observations are the only existing alternate source of forcing data, the NWM is believed to consistently provide the best representation of hydrologic forcing for the LCRR hydrodynamic model. NWM nowcast results from periods without available observations show a diminished response to high-flow conditions, and high-flow events were also underestimated in NWM forecasts, suggesting there is an overall tendency toward a negative bias in the streamflow data used to force the LCRR hydrodynamic model.

3.2 Wind Validation

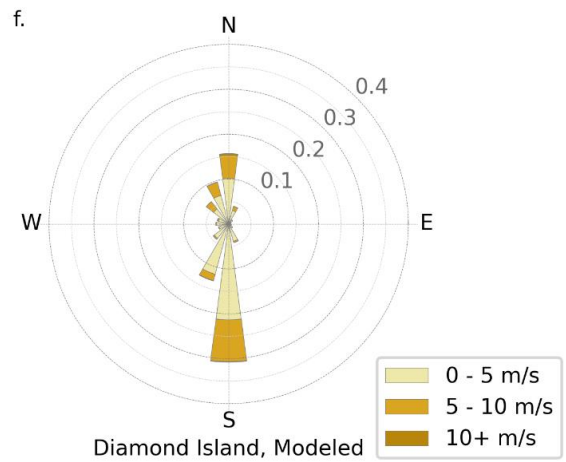
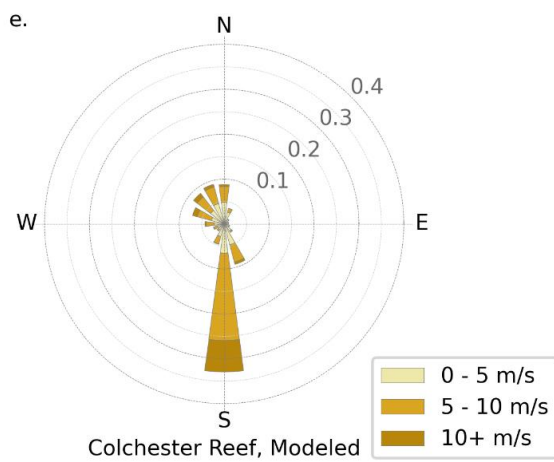
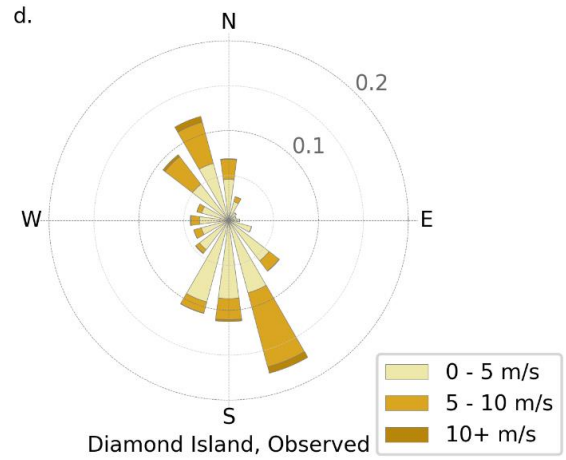
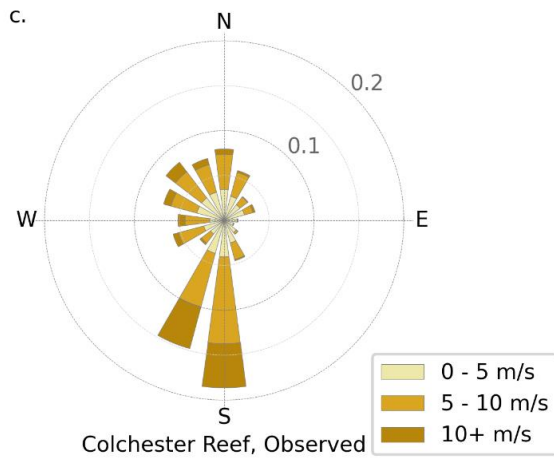
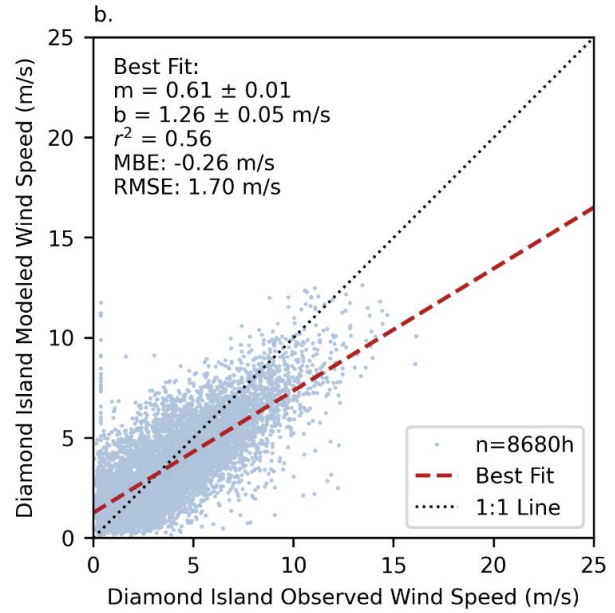
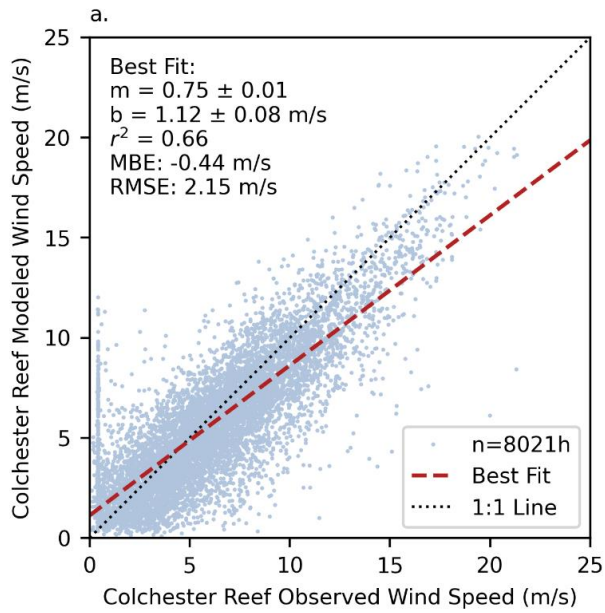


Fig. 5 Wind Nowcast Skill Assessment. Linear regressions of hourly wind speed for HRRR nowcast model against FEMC observations at Colchester Reef (a) and Diamond Island (b), including hourly data points and best fit lines. Wind roses showing the distribution of wind direction (direction wind is from) are shown for the HRRR nowcast model and FEMC observations at Colchester Reef (c and e, respectively) and Diamond Island (d and f, respectively), with the directional bars shaded by the distribution of wind speeds in that direction

Regression analyses conducted between modeled and observed wind speed show a tendency for HRRR to underpredict winds relative to observations, particularly during periods of stronger wind (Fig. 5a-b). Wind roses showing the distribution of winds at each station for both the HRRR nowcast forcing data and the FEMC observations are shown in Fig. 5c-f. At both stations, there is a tendency toward wind movement more-directly from the south in the HRRR nowcast data, whereas FEMC observations show a more variable distribution of southerly wind directions, with Colchester Reef winds often exhibiting a westerly component and Diamond Island winds often exhibiting an easterly component. During times that wind direction has a northerly component, the directional distribution is variable; there is a westerly component at Colchester Reef in both the model data and the observations, while at Diamond Island the winds have a tendency to move from due north in the model and from the northwest in the observations.

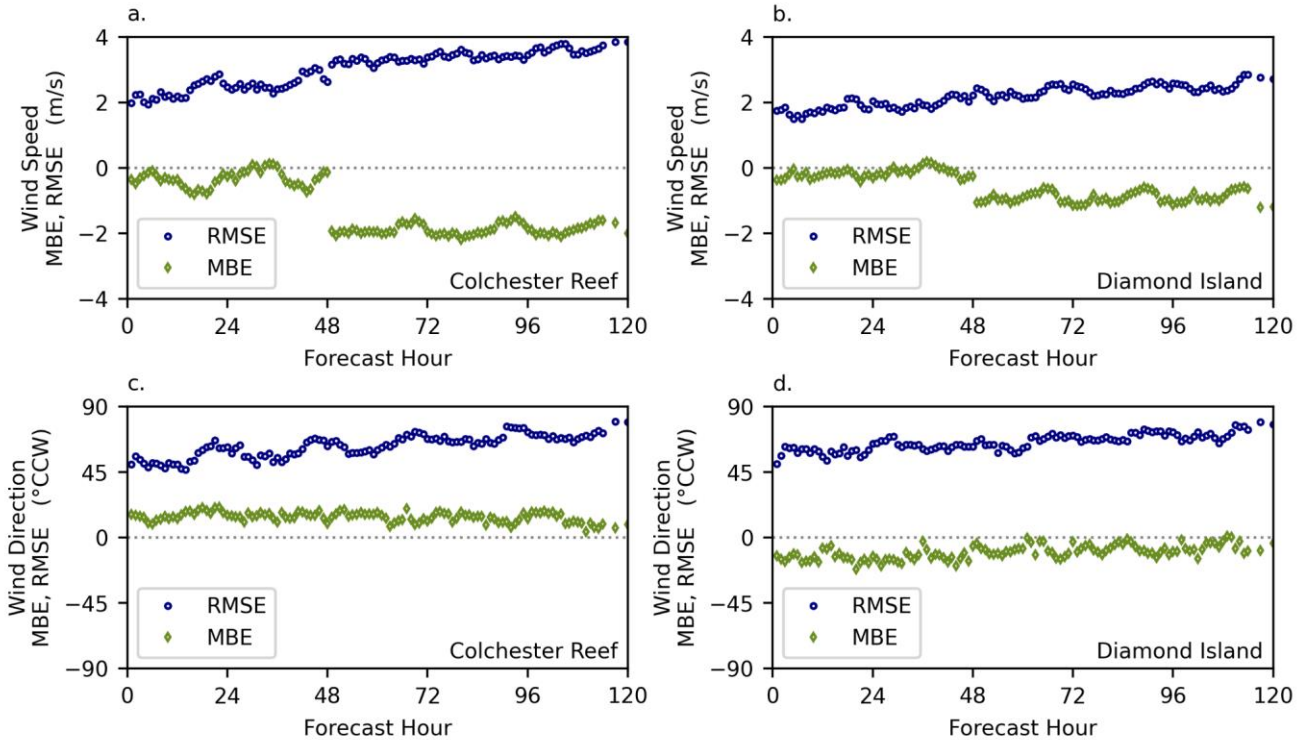


Fig. 6 Wind Forecast Skill Assessment. RMSE (circles) and MBE (diamonds) for wind speed by forecast horizon at Colchester Reef (a) and Diamond Island (b), and for wind direction at Colchester Reef (c) and Diamond Island (d), calculated by comparing wind forecasts derived from the HRRR (first 48 hours) and GFS (last 72 hours) forecast models to FEMC observations

Skill assessment of the wind data used in the model show a tendency toward a negative bias in wind speed at both stations, relative to the FEMC observations (Fig. 6a-b). In addition, there is a step change in MBE values, whereby MBE is greater in magnitude for forecast horizons longer than 48 hours. This step change corresponds to the portions of the forecast that are sourced from HRRR forecasts (hours 0-48) as opposed to 6-hour-old GFS forecasts (hours 49-120), and indicates that there is a greater negative bias in GFS wind speeds than in HRRR wind speeds. At Colchester Reef, the average MBE for the HRRR and GFS portions of the forecast are -0.33 m/s and -1.89 m/s, respectively; similarly at Diamond Island, the MBE increases in

1
2
3
4 magnitude from -0.16 m/s for the HRRR portion of the forecast to -0.91 m/s for the GFS portion of the forecast. There is no
5 step change in RMSE during the forecast window, with Colchester Reef showing a relatively steady increase of RMSE from
6 2.34 m/s to 3.64 m/s when averaged over the first and last 24 hours of the forecast, respectively, and RMSE at Diamond
7 Island steadily increasing from 1.80 m/s to 2.53 m/s over the same windows.
8

9 Skill assessment of wind direction reveals a counter-clockwise (CCW) bias in modeled wind direction at Colchester Reef and
10 a clockwise (CW) bias in modeled wind direction at Diamond Island, relative to observations (Fig. 6c-d). Unlike in the wind
11 speed analysis, no clear step change in direction is present in MBE or RMSE statistics at the 48-hour forecast horizon, when
12 the source of modeled wind data switches from HRRR to GFS. The directional MBE is slightly higher in magnitude during
13 the HRRR portion of the forecast (15.2° CCW at Colchester Reef; 13.7° CW at Diamond Island) than the GFS portion (13.2°
14 CCW at Colchester Reef; 7.6° CW at Diamond Island). Both stations show a steady increase in RMSE over the forecast,
15 with values at Colchester Reef increasing from 54.4° to 70.7° averaged over the first and last hours of the forecast,
16 respectively, and values at Diamond Island increasing from 61.1° to 68.7° over the same periods.
17
18

19 Skill assessment of the wind data demonstrates an overall negative bias in modeled wind speed at both stations analyzed, and
20 a general decline in forcing data skill at longer forecast horizons. Skill during the portions of the forecast forced by HRRR is
21 generally higher than in the portions forced by GFS. This is most noticeable in the wind speed component of the analysis,
22 but is also seen through an increase in directional RMSE from the HRRR portion to the GFS portion of the forecast, despite a
23 modest improvement in MBE in the GFS portion at both stations. A negative bias in Lake Champlain wind forecasts has
24 previously been identified in other models, including the US Short Range Ensemble Forecasting System (SREF), the
25 Canadian High-Resolution Deterministic Prediction System (HRDPS), the Regional Deterministic Prediction System
26 (RDPS), and Regional Ensemble Prediction System (REPS) (Fortin et al. 2015).
27
28
29
30
31
32
33
34
35
36
37
38
39
40
41
42
43
44
45
46
47
48
49
50
51
52
53
54
55
56
57
58
59
60
61
62
63
64
65

3.3 Water Level Skill Assessment

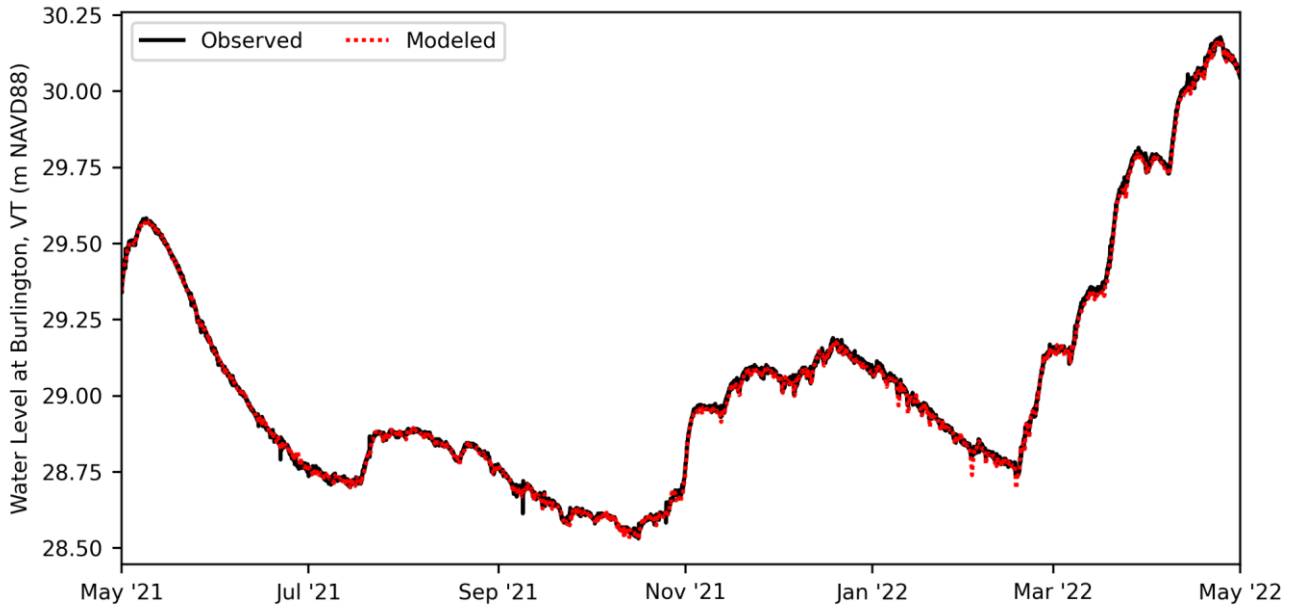


Fig. 7 Lake Champlain annual water level. Time-series of Lake Champlain hourly water level over the skill assessment period at Burlington VT from USGS observations (solid) and the LCRR FVCOM hydrodynamic nowcast model (dashed)

The water level over the course of the skill assessment period is shown in Figure 7 for the Burlington VT gauge location. Because Burlington is centrally located in the basin and relatively sheltered from wind-driven storm surge effects, water level measurements at gauge provide a reasonably representative water level value for the lake. The skill assessment period includes both the 2021 and 2022 spring water level peaks, occurring on May 8-9 and April 24, respectively. The overall range in water levels at the Burlington station during the skill assessment period was 1.649 m, rising from a low of 28.532 m on October 16, 2021 to high of 30.181 m on April 24, 2022. The modeled annual signal shows strong agreement with observations. This is largely attributable to the water level nudging method developed for the LCRR modeling system, which mitigates persistent domain-wide water level drift and prevents such errors from compounding over time.

1
2
3
4
5
6
7
8
9
10
11
12
13
14
15
16
17
18
19
20
21
22
23
24
25
26
27
28
29
30
31
32
33
34
35
36
37
38
39
40
41
42
43
44
45
46
47
48
49
50
51
52
53
54
55
56
57
58
59
60
61
62
63
64
65

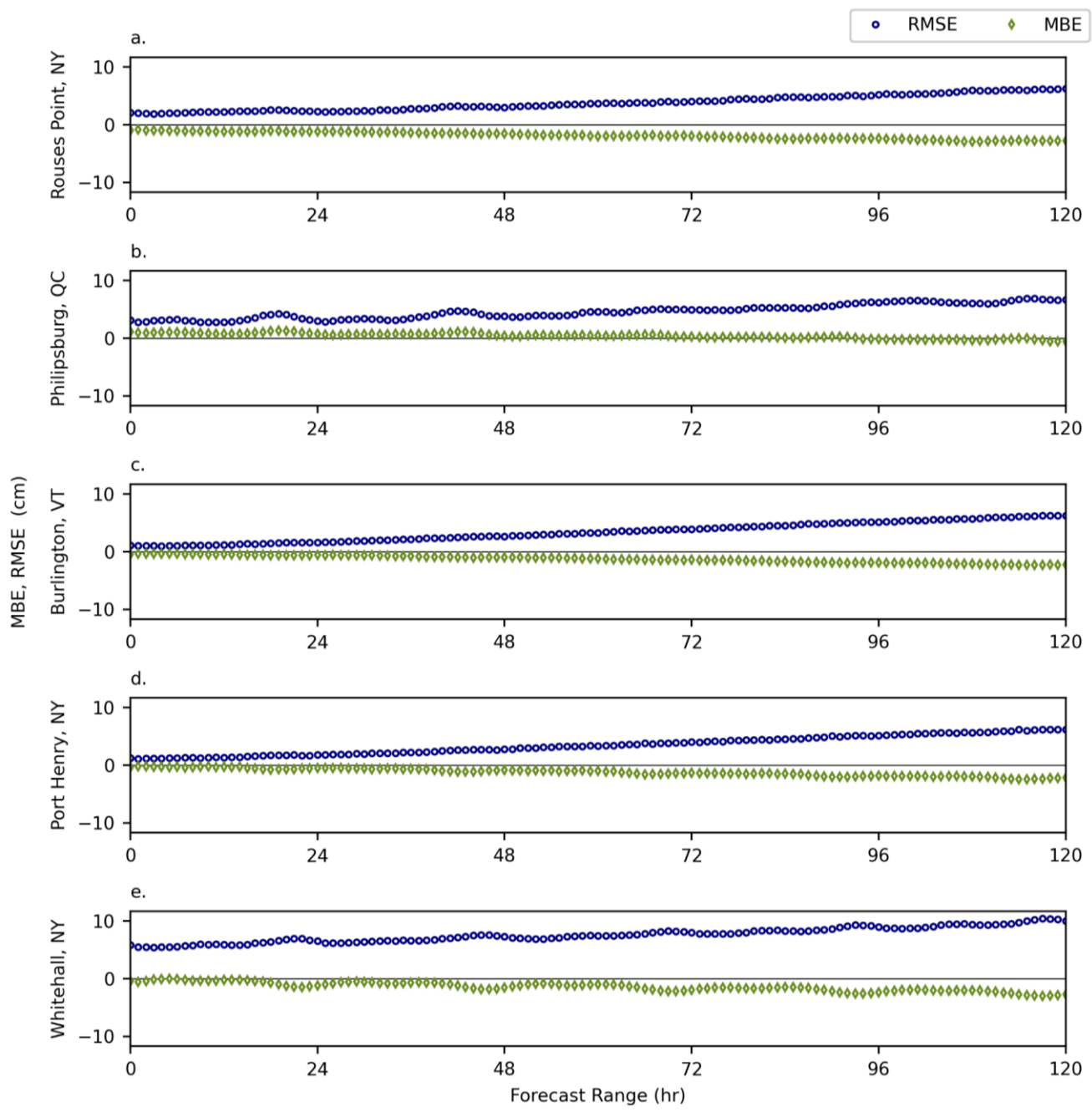


Fig. 8 Water Level Forecast Skill Assessment. RMSE (circles) and MBE (diamonds) for water level by forecast horizon at (a) Rouses Point NY, (b) Philipsburg QC, (c) Burlington VT, (d) Port Henry NY, and (e) Whitehall NY, calculated by comparing river forecasts derived from the LCRR hydrodynamic model to corresponding USGS or ECCC gauge observations

Results from the skill assessment of water levels from the FVCOM hydrodynamic model are summarized in Figure 8 for all five gauge locations analyzed. Modeled water levels show strong agreement with gauge observations at the 0-hour (nowcast) horizon, with MBE values ranging from -0.37 cm at Port Henry NY to +1.13 cm at Philipsburg QC, and RMSE values ranging from 1.09 cm at Burlington VT to 5.85 cm at Whitehall NY. Skill in the water level results shows a gradual, mostly linear decline over the forecast window, with MBE values at the 120-hour forecast horizon ranging from -0.54 cm at

1
2
3
4
5
6
7
8
9
10
11
12
13
14
15
16
17
18
19
20
21
22
23
24
25
26
27
28
29
30
31
32
33
34
35
36
37
38
39
40
41
42
43
44
45
46
47
48
49
50
51
52
53
54
55
56
57
58
59
60
61
62
63
64
65

Philipsburg QC to -2.76 cm Rouses Point NY, and RMSE values ranging from 6.23 cm at Port Henry NY to 10.05 cm at Whitehall NY. The relatively low RMSE values at shorter forecast horizons are indicative of an accurate response to wind-driven storm surges, owing to both the accuracy of the HRRR wind forcing and the FVCOM hydrodynamic simulation.

3.4 Wave Height Skill Assessment

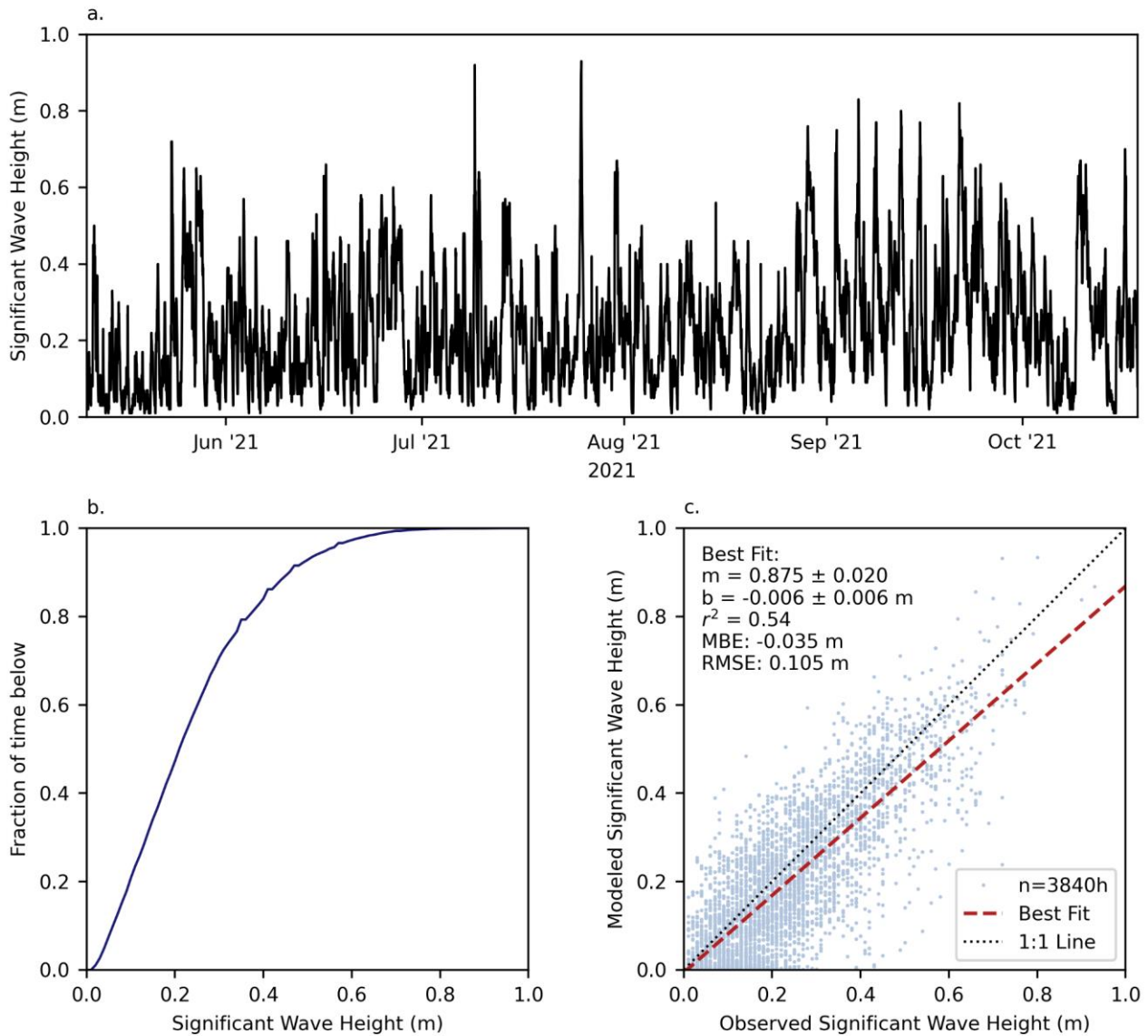


Fig. 9 Wave Nowcast Skill Assessment. (a) Time-series of 30-minute significant wave height from the Lake Champlain DW4 buoy 2021 deployment, and (b) the corresponding cumulative distribution plot. (c) Linear regressions significant wave height for LCRR WW3 modeled values against measurements from the DW4 buoy over the 2021 deployment period, including hourly data points and best fit line

Significant wave height observations from the Lake Champlain DW4 buoy 2021 deployment are shown in Figure 9a-b, and are compared to corresponding model results in Figure 9c. Waves were higher than 0.5m during several events, but did not exceed 1m during the deployment period. Wind speeds were generally higher at the FEMC stations during the fall and winter (not shown), suggesting that the moderate wave conditions observed during the deployment period may be a result of the timing of the deployment, and that larger waves may form during other seasons. Modeled wave heights from the WW3 nowcast cycle show general agreement with observations, with an r^2 value of 0.54, MBE of -3.5 cm, and RMSE of 10.5 cm.

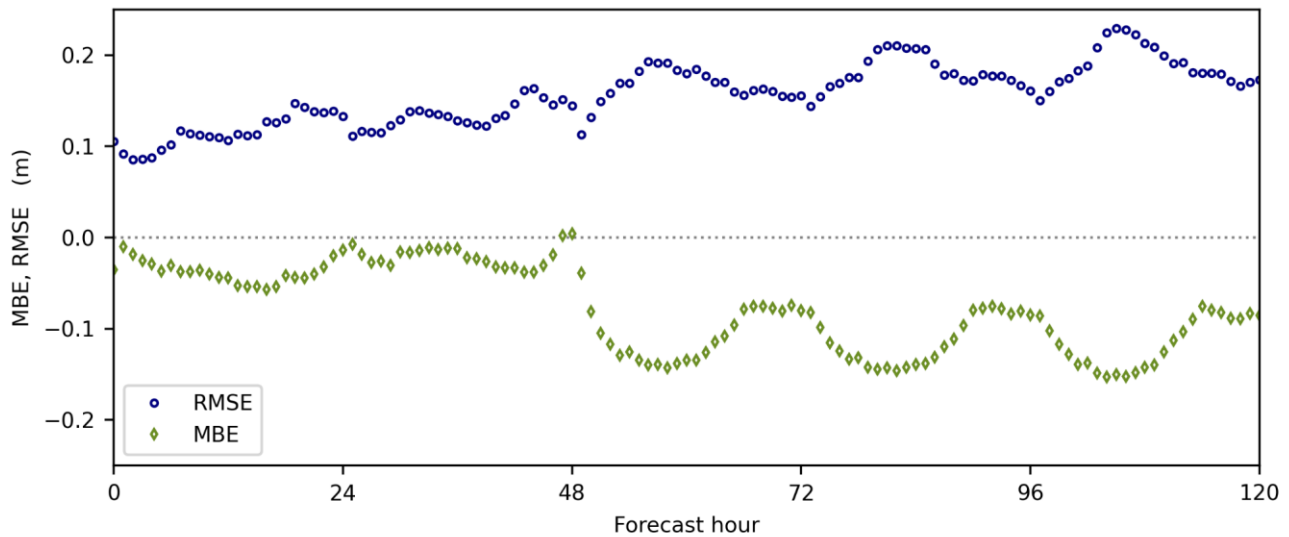


Fig. 10 Wave Forecast Skill Assessment. RMSE (circles) and MBE (diamonds) for significant wave height by forecast horizon at the Lake Champlain DW4 buoy location, calculated by comparing river forecasts derived from the LCRR hydrodynamic model to corresponding USGS or ECCC gauge observations

Skill assessment of wave height forecasts (Fig. 10) show a gradual increase in RMSE over the forecast window, and a step change increase in MBE magnitude at 48 hours, when the forcing data source switches from HRRR to GFS in the forecasts. The RMSE increases from 11.5 cm averaged over the first 24 hours of the forecast to 18.8 cm averaged over the final 24 hours of the forecast. The average MBE over the first 48 hours of the forecast forced by HRRR is -2.9 cm, and the average MBE over the latter 72 hours of the forecast forced by GFS is -11.1 cm. These metrics from both the nowcast and forecast cycles indicate a tendency for the model to underestimate wave heights, which is consistent with the negative biases identified in wind speeds. There is a strong 24-hour periodicity in the wave forecast skill metrics, which is further discussed in Section 4.

4. Discussion and Conclusions

The IJC conducted the LCRR study to explore solutions to the binational issue of flooding in the flood-prone Lake Champlain basin, following the devastating impacts of the record-breaking 2011 flood. Among the final recommendations of the study was that wind-driven impacts on water levels and waves be incorporated in short-term forecasts (ILCRRSB 2022). The LCRR real-time flood forecasting modeling system addresses this critical need, and improves upon existing 1D flood forecasting systems in the region. While there has been some previous work to develop hydrodynamic models for Lake Champlain, the LCRR modeling system is the first comprehensive coastal ocean modeling system for the region that utilizes operational atmospheric and hydrologic models as inputs to a linked hydrodynamic-wave modeling system to produce real-time nowcast and forecast guidance for water levels and waves.

The NWM domain was expanded to cover the full Lake Champlain watershed as part of the study, and use of the NWM inflows as hydrologic forcing allows for a full accounting of hydrologic inputs to the system. This is crucial in a flashy system like Lake Champlain, and is an improvement over models such as the Great Lakes Operational Forecasting System, for which hydrologic inputs are limited to major rivers with gauged flow. Skill assessment of the NWM shows strong agreement with gauge observations for the nowcast cycle, though there is an increasing negative bias at longer forecast horizons. The NOAA operational HRRR and GFS models are used for wind and precipitation forcing in the models and show a general agreement with observations. A negative bias was identified in wind speeds from both of the models, which is more pronounced in the GFS.

1
2
3
4 Water level output from the FVCOM hydrodynamic model provides skillful predictions at the five stations for which
5 comparisons were made. The LCRR modeling system demonstrates capability in simulating both the fluctuations in
6 lakewide water level at seasonal to annual scales, as well as localized wind-driven spatial variability in water level at short-
7 time time scales. MBE values at all five skill assessment locations trend in a negative direction as the forecast horizon is
8 extended, and all five locations have a negative bias at the 120-hour forecast horizon (Fig. 8). The magnitude of this decline
9 in MBE over the 5-day forecast window is comparable among stations, ranging from 1.67 cm to 1.82 cm at all stations except
10 Whitehall NY, for which the magnitude is 2.30 cm.
11
12

13 This consistent trend toward more negative water level bias at longer forecast horizons suggests a tendency of the
14 hydrodynamic model to overestimate hydrological outputs and/or underestimate hydrologic inputs, and is likely due to
15 imperfect hydrologic forcing. Because no forecast data is available for the Richelieu River outflow, the most recent
16 observation of river stage is persisted through the forecast, which may result in the model overestimating outflow at the open
17 boundary during periods of rapid water level rise. In addition, a negative bias was identified in the NWM data used to force
18 inflows in the hydrodynamic model. The average MBE value in NWM inflows at the 120-hour forecast horizon is -65.31
19 m³/s (Fig. 4). When divided by the wet area of the LCRR domain (1.145 x 10⁹ m²), the negative bias in NWM inflow data
20 would result in a deficit in water volume of approximately 0.493 cm per day, or 2.46 cm over a 5-day forecast, which is
21 comparable to the decline in water level MBE. While the inflow deficit calculated in the NWM skill assessment is not
22 directly equivalent to the inflow deficit in the model, due to only the subset of gauged features being used in the former, that
23 these values are comparable suggests that the negative bias in water levels in the LCRR FVCOM hydrodynamic model can
24 largely be accounted for through the negative bias in NWM inflows.
25
26
27

28 Wave height predictions from the WW3 wave model show a general agreement with observations from the DW4 buoy
29 deployed in the main basin of Lake Champlain as a component of this work (Fig. 9c). Wave height predictions show a higher
30 degree of skill during the first 48 hours of the forecast, when they are forced by the HRRR model output (Fig. 10c). In order
31 to understand how the negative bias in waves is impacted by the negative bias in wind forcing, the simple empirical wind-
32 wave relationship developed by Donelan (1980) for fetch-limited waves in the Great Lakes can be applied (Choi et al. 2018):
33
34

$$H_s = 0.00366 g^{-0.62} U^{1.24} F^{0.38} \quad \text{Eqn. 3}$$

35
36 where H_s is the significant wave height (m), U is the wind speed (m/s), F is the fetch length (m), and g is gravitational
37 acceleration (9.81 m/s²). Based on the central location of the DW4 buoy in the main basin of the lake, a nominal fetch value
38 of 2.5×10^4 m (25 km) can be used in the equation, which is the approximate distance of the buoy from Thompson Point to
39 the south and from Cumberland Head to the north (Fig. 1). The average observed and modeled winds during the nowcast
40 cycle were 6.25 m/s and 5.81 m/s, respectively, for which the Donelan 1980 wind-wave relationship yields significant wave
41 height estimates of 0.404 m and 0.369 m, respectively. The difference between these estimates is 3.5 cm, which is consistent
42 with the 3.5 cm negative bias in the wave model (Fig. 9c).
43
44

45 There is a 24-hour periodicity forecast skill metrics, which is most noticeable in the wave height skill assessment (Fig. 10),
46 but is also present in the skill metrics for the wind forecast (Fig. 6) and the water level forecast (Fig. 8). In the case of water
47 level, the signal is strongest in stations at the northern or southern ends of the lake (e.g. Philipsburg QC, Whitehall NY) and
48 is of opposing face at the north end of the lake, relative to the south. Preliminary analysis has revealed a diurnal pattern in
49 the meridional component of wind velocity within the FEMC observations that may not be well-replicated in HRRR and GFS
50 modeled winds used as forcing in the models. As a result, there may be a diurnal water level setup and a diurnal peak in
51 wave energy occurring on the lake that are not represented in the respective models. This diurnal signal is likely orographic
52 in nature, resulting from Lake Champlain's mountainous setting, and additional characterization may be warranted.
53
54

55 Overall, the biases identified in water level results from the FVCOM hydrodynamic model and in wave height results from
56 the WW3 wave model are consistent with the biases identified in model forcing. There is a tendency toward a negative bias
57 in water level at longer forecast horizons, which is consistent with a negative bias in NWM streamflow. Similarly, there is a
58 negative bias in wave height predictions, particularly under higher-wave conditions, which is consistent with a negative bias
59
60
61
62
63
64
65

1
2
3
4 in wind speeds. This suggests that any improvements to the models used as forcing in the LCRR modeling system will have
5 a positive improvement on model performance.
6

7 Future work is needed to develop the baroclinic temperature component of the hydrodynamic model, and to improve
8 representation of winter conditions throughout the LCRR modeling system. Preliminary evaluation was conducted to run the
9 FVCOM hydrodynamic model in a 3D baroclinic mode; however, it was found that the steep bathymetry and narrow
10 morphology of the lake produced unrealistic vertical mixing, thus precluding the formation of a stable thermocline. This
11 demonstrates that while coastal ocean models can be readily applied to some aspects of inland lake domains, such as the wind
12 setup critical to the flood forecasting application, unique challenges remain to be addressed in applying these models to non-
13 traditional domains. In addition, ice cover is unrepresented in the FVCOM hydrodynamic model and coarsely represented in
14 the WW3 wave model, which may limit the accuracy of these models during the winter when ice is present in the domain. In
15 the future, higher-resolution operational ice datasets may be available through advancements in remote sensing.
16

17 Alternatively, development of the baroclinic temperature component in the FVCOM model would allow for dynamic ice
18 modeling through a coupled ice model, such as the Los Alamos Sea Ice model (CICE), as is done in the Great Lakes
19 (Anderson et al. 2018).
20

21
22 The development and validation work described here demonstrates that the LCRR real-time flood forecasting modeling
23 system is capable of providing valuable real-time guidance to forecasters in the Lake Champlain Basin, and serves as a
24 precursor to the first operational hydrodynamic-wave forecasting system for the domain. Output from the LCRR modeling
25 system produces predictions about not just when the lake may reach flood stage, but when and where impacts may be most
26 severe. Specifically, it provides advanced warning as to the magnitude of enhanced impacts as a result of wind-driven storm
27 surges and waves, which are not currently forecast in Lake Champlain. Such guidance could be used in conjunction with
28 high-resolution flood maps to provide detailed warnings to residents, and make informed decisions about evacuations and
29 other safety precautions or property protection measures.
30
31
32

33 *Data availability*

34
35 The modeling datasets generated during the study are available from the corresponding author on reasonable request. Data
36 from the Datawell Directional Waverider 4 buoy are available at the National Data Buoy Center
37 (<https://www.ndbc.noaa.gov/>).
38
39
40

41 *References*

- 42
43 Anderson EJ, Fujisaki-Manome A, Kessler J, Lang GA, Chu PY, Kelley JGW, Chen Y, Wang J (2018) Ice Forecasting in the
44 Next-Generation Great Lakes Operational Forecast System (GLOFS). *J Mar Sci Eng* 6(4):123.
45 <https://doi.org/10.3390/jmse6040123>
46
47 Beletsky D, Titze D, Kessler J, Mason LA, Fry L, Read L, Saunders W, Chu P, Feyen J, Lee D, Kelly JGW, Chen Y, Van der
48 Westhuysen A (2022) Development of Coupled Hydrologic-Hydrodynamic-Wave Flood Forecasting System for Lake
49 Champlain. NOAA Tech. Memo. GLERL-179. NOAA, Great Lakes Environmental Research Laboratory, Ann Arbor,
50 Michigan. <https://doi.org/10.25923/2hy2-ca15>
51
52 Bjerklie DM, Trombley TJ, Olson SA (2014) Assessment of the spatial extent and height of flooding in Lake Champlain
53 during May 2011, using satellite remote sensing and ground-based information: US Geological Survey Scientific
54 Investigations Report 2014-5163. <http://dx.doi.org/10.3133/sir20145163>
55
56 Boudreau P, Cantin JF, Bouchard A, Champoux A, Fortin P, Fiset JM, Fortin N, Thérien J, Morin G (2015) Development of
57 an experimental 2D hydrodynamic model of Lake Champlain using existing bathymetric data. Technical report prepared by
58
59
60
61
62
63
64
65

1
2
3
4 Environment Canada for the International Lake Champlain – Richelieu River Technical Working Group. Lake Champlain-
5 Richelieu River 2D Hydrodynamic Model (H2D2).
6
7 Campbell MK, White JM (2020) Hydrodynamic Modeling of Lake Champlain: Current Resources, Major Gaps. Lake
8 Champlain Basin Program and Lake Champlain Sea Grant.
9
10 Chen C, Beardsley RC, Cowles G (2006) An unstructured grid, finite volume coastal ocean model (FVCOM) system. *J*
11 *Oceanogr* 19:78-89. <https://doi.org/10.5670/oceanog.2006.92>
12
13 Chen C, Beardsley RC, et al. (2013) An unstructured grid, finite-volume coastal ocean model: FVCOM user manual, Fourth
14 Edition. SMAST/UMASSD-13-0701.
15
16 Choi BY, Jo HJ, Lee KH, Byoun DH (2018) Development of Wind Induced Wave Predict Using Revisited Methods. *J Adv*
17 *Res Ocean Eng* 4(3):124-134.
18
19 Chu PY, Kelley JGW, Mott GV, Zhang A, Lang GA (2011) Development, implementation, and skill assessment of the
20 NOAA/NOS Great Lakes Operational Forecast System. *Ocean Dyn* 61(9):1305-16. [https://doi.org/10.1007/s10236-011-](https://doi.org/10.1007/s10236-011-0424-5)
21 [0424-5](https://doi.org/10.1007/s10236-011-0424-5)
22
23 Cosgrove B, Gochis D, Clark EP, Cui Z, Dugger AL, Feng X, Karsten LR, Khan S, Kitzmiller D, Lee HS, Liu Y, McCreight
24 JL, Newman AJ, Oubeidillah A, Pan L, Pham C, Salas F, Sampson KM, Sood G, Wood A, Yates DN, Yu W (2016) An
25 Overview of the National Weather Service National Water Model. American Geophysical Union Fall Meeting 2016 Abstract
26 H42B-05.
27
28 Donelan MA (1980) Similarity theory applied to the forecasting of wave heights, periods and directions. National Water
29 Research Institute.
30
31 Dowell DC, Alexander CR, James EP, Weygandt SS, Benjamin SG, Manikin GS, Blake BT, Brown JM, Olson JB, Hu M,
32 Smirnova TG (2022) The High-Resolution Rapid Refresh (HRRR): An hourly updating convection-allowing forecast model.
33 Part 1: Motivation and system description. *Weather Forecast* 37(8):1371–1395. <https://doi.org/10.1175/WAF-D-21-0151.1>
34
35 Environment and Climate Change Canada (ECCC) (2022) Hydrometric Data. <https://wateroffice.ec.gc.ca>. Accessed
36 September 2022.
37
38 Environmental Modeling Center (EMC) (2022) EMC Operational Wave Models. <https://polar.ncep.noaa.gov/waves>.
39 Accessed September 2022.
40
41 Flynn RH, Rydlund PH Jr, Martin DJ (2016) Network global navigation satellite system surveys to harmonize American and
42 Canadian datums for the Lake Champlain Basin. US Geological Survey No 2016-5009.
43 <http://dx.doi.org/10.3133/sir20165009>
44
45 Forest Ecosystem Management Cooperative (FEMC) (2022) FEMC Data Archive. <https://www.uvm.edu/femc/data>.
46 Accessed September 2022.
47
48 Fortin V, Gaborit E, Dimitrijevic M (2015) Assessing the skill of weather forecasts for the purpose of flood forecasting in
49 Lake Champlain and Richelieu River. Technical report prepared for the International Lake Champlain – Richelieu River
50 Technical Working Group. August 31, 2015.
51
52 Global Systems Laboratory (GSL) (2022). The High-Resolution Rapid Refresh (HRRR). <https://rapidrefresh.noaa.gov/hrrr>.
53 Accessed September 2022.
54
55 Herdman L, Manley T, Mehler P, Kernkamp H (2019) Causeways and Circulation in Lake Champlain. Presented to the
56 International Association of Great Lakes Research. June 2019.
57
58
59
60
61
62
63
64
65

1
2
3
4 International Lake Champlain-Richelieu River Study Board (ILCRRSB) (2019) The Causes and Impacts of Past Floods in the
5 Lake Champlain-Richelieu River Basin, Historical Information on Flooding: A Report to the International Joint Commission.
6 December 2019.
7
8 International Lake Champlain-Richelieu River Study Board (ILCRRSB) (2022) Development of a Binational Flood
9 Forecasting and Real-time Flood Plain Mapping System for Operational Implementation: A Report to the International Joint
10 Commission. June 2022.
11
12 James EP, Alexander CR, Dowell DC, Weygandt SS, Benjamin SG, Manikin GS, Brown JM, Olson JB, Hu M, Smirnova
13 TG, Ladwig T (2022) The High-Resolution Rapid Refresh (HRRR): An Hourly Updating Convection-Allowing Forecast
14 Model. Part 2: Forecast Performance. *Weather Forecast* 37(8):1397-1417. <https://doi.org/10.1175/WAF-D-21-0130.1>
15
16 Kelley JGW, Chen Y, Anderson EJ, Lang GA, Xu J (2018). Upgrade of NOS Lake Erie Operational Forecast System
17 (LEOFS) to FVCOM : model development and hindcast skill assessment. United States Coast Survey Development
18 Laboratory. NOAA technical memorandum NOS CS 40. <http://doi.org/10.7289/V5/TM-NOS-CS-40>
19
20 Kelley JGW, Chen Y, Anderson EJ, Lang GA, Peng M (2020) Upgrade of NOS Lake Michigan and Lake Huron operational
21 forecast systems to FVCOM : model development and hindcast skill assessment. United States Coast Survey Development
22 Laboratory. NOAA technical memorandum NOS CS 42. <https://doi.org/10.25923/mmyb-qh56>
23
24 Lake Champlain Basin Program (LCBP) (2013) Flood Resilience in the Lake Champlain Basin and Upper Richelieu River.
25
26 Marti CL, Schroth AW, Zia A (2019) Physical and biogeochemical processes across seasons in Missisquoi Bay, Lake
27 Champlain: Insights from a three-dimensional model. American Geophysical Union Fall Meeting December 2019 Abstract
28 H34C-04.
29
30 McKay L, Bondelid T, Dewald T, Johnston J, Moore R, Rea A (2012) NHDPlus Version 2: User Guide.
31
32 Mendelsohn D, Isaji T, Rines H (1995) Hydrodynamic and water quality modeling of Lake Champlain. Report to Lake
33 Champlain Management Conference. 1995.
34
35 Mendelsohn D, Swanson C, Isaji T (1997) Hydrodynamic modeling of Missisquoi Bay in Lake Champlain. Final report
36 submitted to Vermont Geological Survey, Vermont Agency of Natural Resources.
37
38 National Centers for Environmental Information (NCEI) (2022) Global Forecast System (GFS).
39 <https://www.ncei.noaa.gov/products/weather-climate-models/global-forecast>. Accessed September 2022.
40
41 Office of Water Prediction (OWP) (2022). The National Water Model. <https://water.noaa.gov/about/nwm>. Accessed
42 September 2022.
43
44 Peng M, Schmalz RA Jr, Zhang A, Aikman F III (2014) Towards the Development of the National Ocean Service San
45 Francisco Bay Operational Forecast System. *J Mar Sci Eng* 2(1):247-286. <https://doi.org/10.3390/jmse2010247>
46
47 Riboust P, Brissette F (2015) Climate change impacts and uncertainties on spring flooding of Lake Champlain and the
48 Richelieu River. *J Am Water Resour Assoc* 51(3):776-793.
49
50 Riboust P, Brissette F (2016) Analysis of Lake Champlain/Richelieu River's historical 2011 flood. *Can Water Resour J* 41(1-
51 2):174-185. <https://doi.org/10.1080/07011784.2014.982190>
52
53 Stickney M, Hickey C, Hoerr R (2001) Lake Champlain basin program: Working together today for tomorrow. *Lakes Reserv:*
54 *Res Manag* 6(3):217-223. <https://doi.org/10.1046/j.1440-1770.2001.00150.x>
55
56 Touma JS (1977) Dependence of the wind profile power law on stability for various locations. *J Air Pollut Control Assoc*
57 27(9):863-866. <https://doi.org/10.1080/00022470.1977.10470503>
58
59
60
61
62
63
64
65

1
2
3
4
5
6
7
8
9
10
11
12
13
14
15
16
17
18
19
20
21
22
23
24
25
26
27
28
29
30
31
32
33
34
35
36
37
38
39
40
41
42
43
44
45
46
47
48
49
50
51
52
53
54
55
56
57
58
59
60
61
62
63
64
65

United States Geological Survey (USGS) (2022) USGS Water Data for the Nation. <https://waterdata.usgs.gov/nwis>. Accessed September 2022.

United States National Ice Center (USNIC) (2008). IMS Daily Northern Hemisphere Snow and Ice Analysis at 1 km, 4 km, and 24 km Resolutions, Version 1. Updated Daily. <https://doi.org/10.7265/N52R3PMC>. Accessed September 2022.

The WAVEWATCH III Development Group (WW3DG) (2019) User manual and system documentation of WAVEWATCH III version 6.07. Tech Note 333, NOAA/NWS/NCEP/MMAB, College Park, MD, USA.

Wei E, Zhang A, Yang Z, Chen Y, Kelley JG, Aikman F, Cao D (2014). NOAA’s Nested Northern Gulf of Mexico operational forecast systems development. *J Mar Sci Eng* 2(1):1-17. <https://doi.org/10.3390/jmse2010001>